Contrasting processes in silicic magma chambers: evidence from very large volume ignimbrites

ERIC H. CHRISTIANSEN*

Department of Geological Sciences, Brigham Young University, Provo, Utah, 84602, USA

Abstract – Very large volume (>1000 km^3 of magma) crystal-rich dacitic ignimbrites that lack pronounced evidence of fractional crystallization or vertical zonation erupt in some continental magmatic arcs (e.g. the Lund Tuff of the Great Basin and the Fish Canyon Tuff of Colorado in western USA). Apparently, their magma chambers were only modestly heterogeneous and not systematically zoned from top to bottom. These ignimbrites have 40 to 50 % phenocrysts set in a high-silica rhyolite glass. Mineral assemblages and mineral compositions suggest pre-eruption temperatures were 730 to 820 °C and water and oxygen fugacities were relatively high. We have speculated that these very large volume ignimbrites are unzoned because crystallization and convection in slab-shaped magma chambers inhibited separation of crystals from liquids and resulted in a chamber filled with compositionally heterogeneous magma that lacked systematic chemical zonation or strong fractionation. However, many other very large volume silicic ignimbrites are strongly fractionated and may be vertically zoned (e.g. tuffs related to the Yellowstone hotspot). These rhyolitic tuffs typically have few phenocrysts, anhydrous mineral assemblages, low oxygen fugacities, crystallization temperatures of 830 to 1050 °C, and a strong imprint of fractional crystallization. Yet these Yellowstone-type rhyolites are derived from chambers 40 to 70 km across which have sill-like shapes (depth/diameter ratios much less than 1). Thus, factors other than chamber shape must be important for establishing the degree of evolution and nature of zonation in silicic magma chambers. Here, the role of crystallinity-dependent viscosity on the evolution of these two types of contrasting magmas is explored. Calculated magma viscosities for the hot, dry, crystal-poor rhyolites are significantly lower than for the cooler, wetter, crystal-rich dacites. Perhaps these hot rhyolites had low enough crystal contents and viscosities to allow efficient crystal–liquid separation, probably by a combination of unhindered crystal-settling, floor crystallization (including compaction), and crystallization on the walls of large chambers. Clean separation of melt from residual solids at their sources may have been promoted by their high temperatures and low viscosities ($< 10^{4.5}$ Pa s). In contrast, monotonous dacitic magmas may never have been crystal-free near-liquidus magmas. Their large magma chambers may have developed by progressive growth at a shallow level with repeated input of intermediate to silicic magma. Crystallization of the water-enriched dacitic magmas occurred at lower temperatures (< 800 °C) where crystallinity and hence magma viscosity ($> 10^{6.5}$ Pa s) were significantly higher. These characteristics inhibited all forms of crystal–liquid separation, hindered development of systematic vertical zonation, and promoted quasi-equilibrium crystallization in small domains within large heterogeneous magma chambers. Eruptions of these crystal-rich dacites may only occur if the roof fails over a growing magma chamber that is becoming increasingly molten.

Keywords: A-type granites, rhyolite, dacite, ignimbrite, magma chambers.

1. Introduction

Several very large volume (> 1000 km^3 of erupted magma) ignimbrites are dacitic and lack the vertical zonation found in many other tuffs. Hildreth (1981) refers to this class of ignimbrites as monotonous inter-mediates because of their intermediate silica contents and nearly uniform chemical and mineralogical char-acteristics. Apparently, their magma chambers were modestly heterogeneous but neither highly evolved nor systematically zoned from top to bottom. Some have

speculated that these very large volume ignimbrites were unable to become highly evolved or composition-ally zoned because convective mixing in slab-shaped magma chambers inhibited separation of crystals from liquids and systematic chemical zonation (Maughan *et al.* 2001; De Silva & Wolff, 1995). In magma cham-bers with pancake shapes, wall crystallization is min-imized. Moreover, evolved buoyant liquids produced by floor crystallization might simply rise and mix with less-evolved magma above them. Cool, dense, crystal-laden plumes falling from the roof of the chamber might mix with magma beneath them. Maughan *et al.* (2001) contrasted this with cylindrical magma chambers where

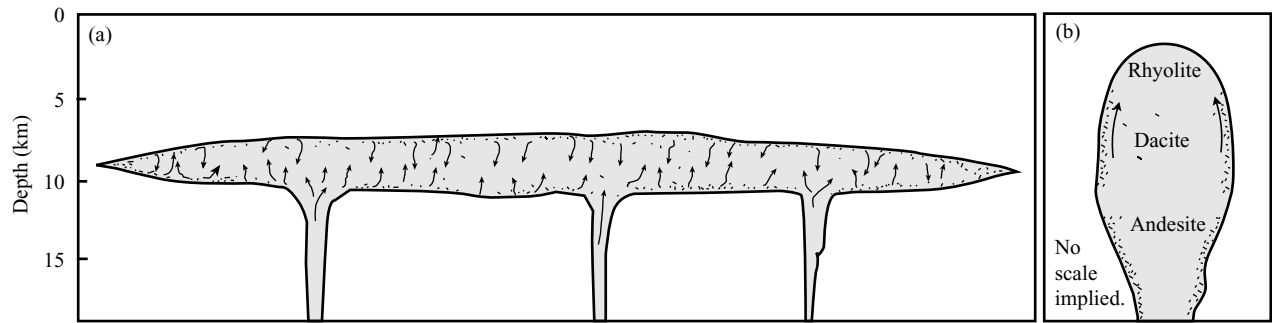* Author for correspondence: eric_christiansen@byu.edu

Figure 1. Magma chamber shapes may affect compositional evolution of magma. (a) Very large volume ignimbrites may be unzoned because replenishment, crystallization and convection in slab-shaped magma chambers inhibit separation of crystals from liquids and result in compositionally heterogeneous chambers that lack systematic chemical zonation. Evolved liquids produced by floor crystallization might simply mix with less-evolved magma above them. Cool, dense, crystal-laden plumes might mix with materials beneath them. (b) Cylindrical magma chambers where crystallization on nearly vertical walls dominates allow evolved less-dense melt to migrate to the top of the chamber. The chamber gradually becomes zoned by fractional crystallization.
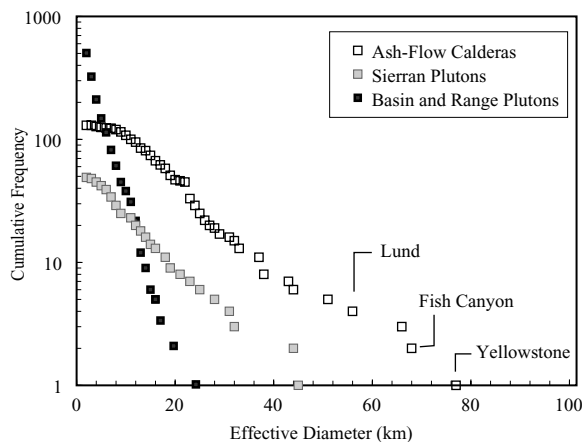

Figure 2. The rhyolite and dacite tuffs discussed here are among the largest on Earth (cf. Mason, Pyle & Oppenheimer, 2004) and were erupted from calderas with effective diameters of 40 to 70 km. These calderas probably reflect the size of the underlying magma chambers and are much larger than typical plutons in arc-related batholiths like the Sierra Nevada or those currently exposed in the Great Basin of Nevada and Utah (J. Radebaugh, unpub. M.Sc. thesis, Brigham Young Univ., 1999).

wall-crystallization dominates, producing chemically evolved less-dense melt that migrates to the top of the chamber. The chamber gradually becomes zoned by fractional crystallization (Fig. 1).

However, many other very large volume ignimbrites are highly evolved rhyolites, some of which are vertically zoned, suggesting that their parent magma chambers were also vertically zoned (e.g. tuffs related to the Yellowstone hotspot). Nonetheless, these very large Yellowstone-type rhyolites must be derived from chambers that are sill-like with low aspect ratios. Their calderas are as large as those for the monotonous dacites, 40 to as much as 70 km across (Fig. 2). This implies that the subjacent magma chambers were approximately this diameter as well. Even if such a magma chamber extended through the entire crust, its height/diameter ratio would still be less than one. Thus,

factors other than chamber shape may also be important for differentiation (or lack thereof) of very large silicic magma chambers.

In this paper, I explore some of these other factors and focus mainly on the roles of composition, temperature and crystallinity, as they relate to the evolving viscosity of a magma system in hindering or allowing the separation of crystals from liquids and controlling the point at which eruptions may occur.

2. Very large volume dacitic ignimbrites

Very large dacitic ignimbrites in the western United States include the Fish Canyon Tuff from Colorado (Whitney & Stormer, 1985; Bachmann, Dungan & Lipman, 2002) and the Cottonwood Wash, Wah Wah Springs and Lund tuffs of the Indian Peak caldera complex (Best, Christiansen & Blank, 1989; Maughan *et al.* 2001) and the Monotony Tuff of the Central Nevada caldera complex (Ekren *et al.* 1971; L. V. Phillips, unpub. Ph.D. thesis, Univ. Georgia, 1989). Figure 3 shows the locations of these Great Basin caldera complexes. For each of these tuffs, the calderas are 50 km or more across (Fig. 2) and outflow deposits extend another 50 to 100 km from the margins of the calderas. The Fish Canyon Tuff, with an estimated eruption volume of 5000 km^3, is one of the largest known eruptions (Mason, Pyle & Oppenheimer, 2004). The Wah Wah Springs and the Lund tuffs have estimated volumes of over 3000 km^3; the caldera for Cottonwood Wash Tuff is probably buried in a Basin and Range graben, but it has an outflow volume of about 1500 km^3. The Andean examples of very large dacitic ignimbrites include the Cerro Galan (Francis *et al.* 1989) and the Atana ignimbrites (Lindsay *et al.* 2001). The Cerro Galan ignimbrite is phenocryst-rich (41–53 %) but lithic- and pumice-poor, has a minimum volume of 1000 km^3, is as thick as 200 m, and extends as much as 100 km in radial directions from the 30 × 50 km resurgent caldera. The dacitic Atana tuff
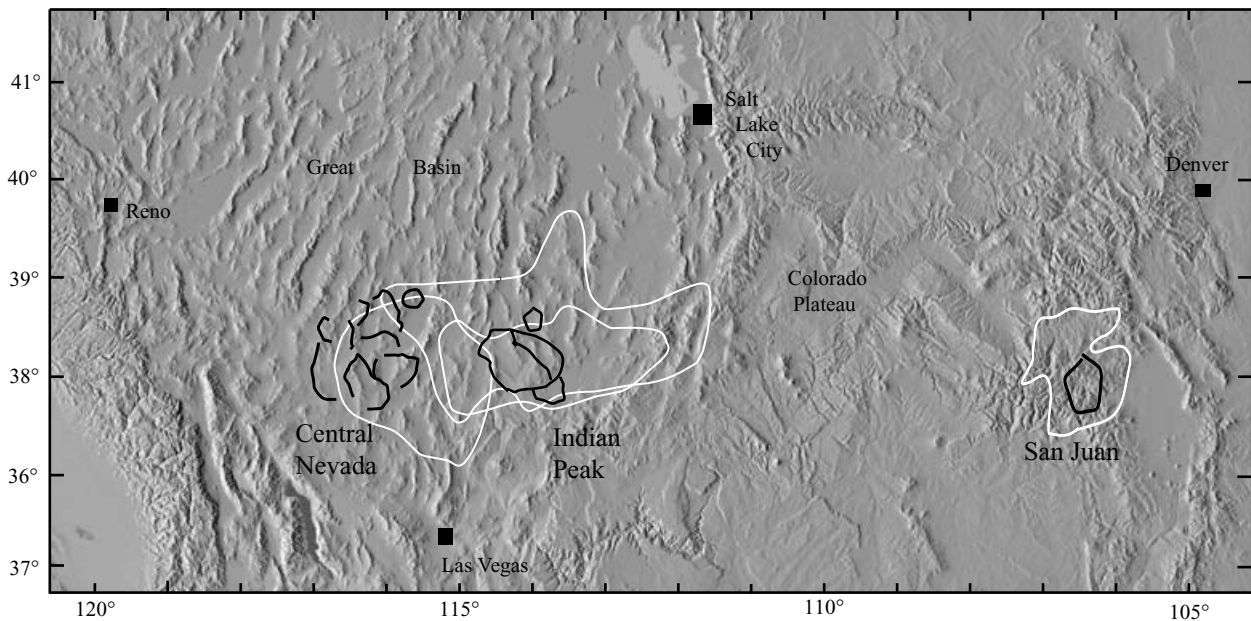
Figure 3. In the western United States, several sheets of crystal-rich dacitic ignimbrites with volumes of several thousand cubic kilometres erupted during Oligocene times. Here the calderas (bold lines) and extent of dacitic ash-flow deposits are shown for the Indian Peak (Wah Wah Springs, Cottonwood Wash and Lund tuffs) and Central Nevada (the Monotony Tuff) caldera complexes. In the Neogene, very large volume, crystal-poor rhyolitic ignimbrites erupted along the Snake River Plain, including those from the Yellowstone caldera and from poorly defined volcanic fields further west.

is similar, with 40 to 50 % crystals set in a rhyolitic glass. It has an estimated volume of 2500 km^3.

These dacitic ignimbrites have 40 to 50 % phenocrysts set in a high-silica rhyolite glass (Table 1). The typical mineral assemblage is plagioclase, quartz, biotite, hornblende, magnetite, ilmenite, pyrrhotite, apatite and zircon; many of these tuffs also include titanite and sanidine and a few have Mg-rich pyroxenes. Experimental work on the Fish Canyon magma (Johnson & Rutherford, 1989) and mineral geothermometry suggest pre-eruption temperatures were 730 to about 820 °C and oxygen and water fugacities were relatively high but fH$_2$O < 1 (Johnson & Rutherford, 1989). A variety of geothermometers show that the Lund Tuff crystallized at 735 to 820 °C and that it was not water-saturated until after eruption commenced (Maughan *et al.* 2001).

Experiments and Al-in-hornblende barometry show the Fish Canyon Tuff (Johnson & Rutherford, 1989), Lund (Maughan *et al.* 2001) and Atana (Lindsay *et al.* 2001) crystallized at about 1.6 to 2.5 kbar. Co-existing Fe–Ti oxides have been used to estimate fO$_2$, which for these magmas is between 2 and 3 log units above the QFM oxygen buffer.

The dominant volumes of these tuffs are high-K dacite. According to the classification of Frost *et al.* (2001), most are magnesian and calc-alkalic or alkalic. Most are metaluminous, but some samples are slightly peraluminous. All are zircon-saturated and have relatively low concentrations of Zr, less than about 200 ppm. Fe$_2$O$_{3T}$ concentrations are about 5 wt % at 65 wt % SiO$_2$. Neither strongly compatible nor incompatible trace elements show large ranges in concentration. For example, Rb in the Lund Tuff has an enrichment factor of about 2 when the most mafic and most silicic pumices are compared. Moreover, vertical sections as thick as 2 km have been sampled that show no systematic chemical or mineralogical zonation and only slight variations throughout the section. Maughan *et al.* (2001) emphasize that small but significant differences in mineral and pumice compositions show that the parent magmas were at least somewhat variable, ranging from 65 to 69 % SiO$_2$, even if the magma chamber was not systematically zoned.

Whitney & Stormer (1985) and Bachmann, Dungan & Lipman (2002) conclude that almost all of the sample to sample variation in the tuffs is the result of variation in the ratio of glass to crystals that was caused by variable winnowing of glass shards during eruption. Glass elutriation during eruption should not affect the compositions of pumice clasts or of mineral compositions. Thus, if these are variable, then it is safe to conclude the parental magma had a variable composition. In fact, pumice clasts in the Cerro Galan ignimbrite show that Rb, Sr and Ba vary by a factor of nearly two and silica ranges from 66 to 70 wt % (Francis *et al.* 1989). In addition, Ross *et al.* (2002) show that pumices from the Cottonwood Wash Tuff have SiO$_2$ contents that range from 65 to 70 wt % SiO$_2$. Mineral compositions tell a similar story. For example, in the Lund Tuff, hornblendes have Fe/(Fe + Mg) ratios that range from 0.38 to 0.44 (Maughan *et al.* 2001) and in the Cottonwood Wash Tuff the ratio ranges from 0.35 to 0.45 (Ross *et al.* 2002). In the 'homogeneous'

Table 1. Comparison of two types of very large volume silicic ignimbrites

	Crystal-poor rhyolites					Crystal-rich dacites					
	Cougar Point Tuff		Tuff of McMullen Creek		Huckleberry Ridge	Lund Tuff			Fish Canyon Tuff		
	Glass	Bulk tuff	Bulk tuff	Glass	Bulk tuff	Bulk tuff	Pumice	Glass	Bulk tuff	Bulk tuff	Glass
SiO_2 (wt %)	75.58	73.30	70.41	74.21	76.00	65.30	66.29	78.17	67.61	64.63	77.19
TiO_2	0.31	0.49	0.71	0.38	0.13	0.68	0.68	0.13	0.46	0.60	0.12
Al_2O_3	12.10	13.00	13.38	13.06	12.82	15.71	15.68	12.51	15.92	17.04	12.51
Fe_2O_3			4.75	2.31		4.99	4.99		3.74	4.75	
FeO	2.08	2.99			1.68			0.56	0.00		0.55
MnO		0.05			0.03	0.08	0.09	0.06	0.08	0.11	0.03
MgO	0.12	0.42	0.55	0.18	<0.10	1.41	1.41	0.11	0.92	1.11	0.11
CaO	0.76	1.35	2.03	1.42	0.66	4.82	3.87	0.95	3.07	3.63	0.60
Na_2O	3.03	2.52	3.24	2.71	3.34	2.80	2.92	2.78	3.92	4.05	2.94
K_2O	5.99	5.78	4.77	5.63	5.33	4.03	3.87	4.73	4.11	4.07	5.95
P_2O_5	0.03	0.09	0.15	0.09	0.01	0.19	0.20		0.18	0.00	
Total	100.00	99.99	100.00	100.00	100.00	100.01	100.00	100.00	100.00	100.00	100.00
Rb (ppm)	165	220	183	200	186	110	116		110		288
Sr	43	87	101	77	21	552	565		487		85
Zr	572	483	571	437	233	206	216		174		79
Ba	983	989	1020	1110	540	933	981		891		478
fO_2	QFM −0.3		~QFM		QFM	QFM +2.8				QFM +2.8	
Pressure (kbar)							2.2			2.4	
Eruption T (°C)	900–970 °C	950°		900°	850–950°	770°				760°	
Phenocrysts (wt %)		10	2–20		2–15	41	55			40	
Sample	95cpt/j10	I-841	GVP01KW	GVP01KG	65YR-3A	COYOT-1E	MLLR-6-65-1A	LAM-5V			
Reference	Cathey & Nash, 2004	Wright, McCurry & Hughes, 2002	Wright, McCurry & Hughes, 2002		Hildreth, Halliday & Christiansen, 1991	Maughan et al. 2001			Bachman, Dungan & Lipman, 2002	Johnson & Rutherford, 1989	Johnson & Rutherford, 1989; Bachman, Dungan & Lipman, 2002

Major element analyses normalized to 100 % volatile free.

Fish Canyon Tuff, Fe/(Fe + Mg) ratios in hornblende range from 0.31 to 0.43 (Bachmann & Dungan, 2002). Apparently, the magma chambers that hosted these crystal-rich dacitic magmas were cool, wet and modestly heterogeneous but not highly evolved nor systematically zoned from top to bottom.

3. Very large volume rhyolitic ignimbrites

Hot and chemically evolved rhyolitic tuffs contrast with the dacites described above. These phenocryst-poor rhyolites typically have strong imprints of fractional crystallization, anhydrous mineral assemblages and eruption temperatures of 850 to over 1000 °C. The very large volume rhyolitic ignimbrites related to the Yellowstone hotspot such as the Cougar Point tuffs (Cathey & Nash, 2004), the tuff of McMullen Creek (Wright, McCurry & Hughes, 2002) and the Lava Creek and Huckleberry Ridge tuffs (Hildreth, Halliday & Christiansen, 1991; Christiansen, 2001) from the Yellowstone caldera show the range of characteristics for this class (Table 1). The Huckleberry Ridge Tuff has a volume of about 2500 km[3] and the Lava Creek has a volume of about 1000 km[3] (Christiansen, 2001). The calderas for most of the other very large tuffs are buried by younger basalt and hence their volumes are difficult to estimate, but Cathey & Nash (2004) estimate from the volume of fallout tuff that the largest of the ten different members of the Cougar Point Tuff has a total erupted volume approaching 1000 km[3]. The hottest ($\sim$ 1050 °C) ignimbrites erupted in the western Snake River Plain; the younger ones near Yellowstone include the coolest ($\sim$ 850 °C) eruptions (Perkins & Nash, 2002). Judging from the comprehensive data set of Perkins & Nash (2002), the average eruption temperature is near 960 °C. Oxygen fugacities are low, typically near the QFM buffer.

The silicic ignimbrites of the Snake River Plain are generally crystal-poor with 0 to 20 % crystals. A typical mineral assemblage is quartz, plagioclase and sanidine or anorthoclase, Fe-rich clino- and orthopyroxenes, apatite, magnetite and ilmenite. Fayalite crystallized in some, but biotite and hornblende are rare. The silicic rocks of the Snake River Plain are high-K rhyolites; dacites are rare. In contrast to the crystal-rich dacites, these rhyolites are ferroan and usually alkalic. Most are metaluminous. Because of their high temperatures, all have rather high concentrations of Zr (200 to 700 ppm) and Fe_2O_{3T} (5.5 % at 70 % SiO_2) compared to the dacites. Enrichment factors for incompatible elements are high in some (Fig. 4), but even more significant are the low concentrations of elements compatible in mafic silicates and oxides (Ni, Cr, Co, Sc, Mg) and in feldspars (Sr, Eu and Ca). The differences between these two different types of silicic magma systems are evident on two element variation diagrams comparing the dacitic Lund Tuff and the rhyolites of the tuff
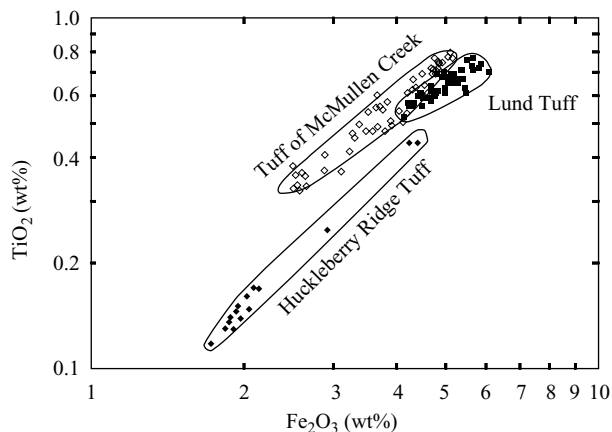

Figure 4. Compositional comparison of Lund Tuff (a large crystal-rich dacite) and two rhyolite tuffs from the Snake River Plain: the tuff of McMullen Creek and the Huckleberry Ridge Tuff. Data from Wright, McCurry, & Hughes (2002), Maughan *et al.* (2001), Hildreth, Halliday & Christiansen (1991) and Christiansen (2001). The rhyolites show extended range of compositions consistent with strong differentiation.

of McMullen Creek and the Huckleberry Ridge Tuff (Fig. 4).

Some of these hot rhyolites show significant vertical zonation (Cathey & Nash, 2004; Hildreth, 1981; Christiansen, 2001). Normal elemental zonation (Fig. 4) with incompatible element-rich tuff at the base and less-enriched tuff at the top is documented for several of the Yellowstone ignimbrites, as is isotopic (Nd, Pb, Sr) zonation (Christiansen, 2001). Most of the tuffs are also zoned with respect to phenocryst proportions: phenocryst-poor bases grade to tops with more phenocrysts (as much as 20 %). However, Wright, McCurry & Hughes (2002) found little evidence for vertical elemental or mineralogical zonation within the McMullen Creek tuff, even though it is compositionally rather variable (Fig. 4).

4. Phenocryst proportions as a function of temperature

In addition to chamber geometry, magma viscosity may play an important role in defining the differences between the monotonous dacites and the highly evolved rhyolites described above. Magma viscosity is a strong function of three interrelated factors: crystal content, temperature and melt composition, especially water content. The effect of these variables can be illustrated by examining the temperature–crystallization relations for magmas with varying water contents. In the absence of experiments showing the temperature–phenocryst relations, the computer program MELTS (Ghiorso & Sack, 1995) was used to estimate crystallization paths. Undoubtedly, the results have significant uncertainties and all of the details will not stand up to experimental investigations. This is particularly true for the hydrous minerals for which the thermodynamic database is
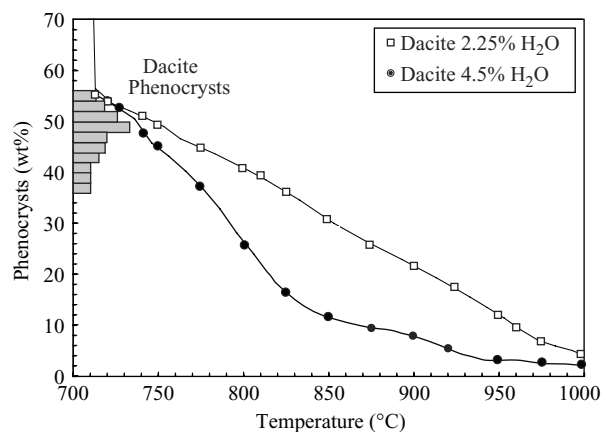
Figure 5. Temperature v. percentage of crystals as calculated for a dacitic magma using MELTS (Ghiorso & Sack, 1995). The conditions assumed for the calculations are given in Table 2. The proportions of crystals in the Lund Tuff and its pumice fragments are shown as a histogram on the left.

Table 2. Input parameters for MELTS models

	Rhyolite	Dacite
SiO_2	71.08	66.72
TiO_2	0.71	0.61
Al_2O_3	13.71	14.82
Fe_2O_3	0.80	1.69
FeO	3.60	3.20
MgO	0.55	1.76
CaO	1.93	4.20
Na_2O	3.10	3.00
K_2O	4.52	4.00
Total	100.00	100.00
fO_2	QFM	QFM + 3
Pressure (kbar)	2	2
Liquidus T (°C)		
1.5 % H_2O	1020°	
2.25 % H_2O		1067°
4.5 % H_2O	985°	1041°
Representative unit	McMullen Creek	Lund Tuff
Eruption T (°C)	990°	773°
Phenocrysts (wt %)	2 to 20	47
Reference	Wright, McCurry & Hughes, 2002	Maughan et al. 2001

Concentrations in wt % normalized to 100 on a volatile-free basis. FeO and Fe_2O_3 calculated at T and fO_2 of interest.

poorly constrained. For example, in these models biotite and amphibole were never in equilibrium and the calculated biotite composition was in all cases a pure Mg end-member, neither of which reflects the real nature of the magma. Nonetheless, appropriate mineral assemblages, temperatures and crystal proportions were found in most of the model calculations. Fortunately, the phenocryst proportions (and hence melt water concentrations) of importance here were relatively insensitive to small changes in starting compositions, including H_2O content and fO_2.

4.a. Crystallization paths for dacite

First, consider the temperature-dependent crystallinity of a dacite with 67 % SiO_2 like the Lund Tuff. Figure 5 shows temperature versus crystal content for two different assumed starting water contents ($H_2O_o = 4.5$ % and 2.25 %) as calculated using MELTS. Both crystallization paths were calculated in equilibrium mode with no separation of crystals from residual liquids. Other details of the model are given in Table 2. Note that for a given temperature, crystal content is significantly higher in the melt with the lower water content. Although there are certain to be discrepancies between the calculated crystal contents and those observed in natural magmas, similar relationships between temperature and crystal content have been found with experiments on natural dacitic compositions (Costa, Scaillet & Pichavant, 2004).

In the calculations for the dacite with 2.25 % H_2O, crystal content correlates smoothly with temperature. Melt water contents are about 3.9 % at 780 °C (Fig. 7), the approximate eruption temperature of the Lund Tuff. At this temperature, the model magma is very similar to the erupted Lund Tuff and has 44 wt % phenocrysts of plagioclase, sanidine, biotite and magnetite.

(Amphibole and quartz crystallize at slightly lower temperatures.) Water saturation occurs when the melt water concentration reaches about 5 wt % at 65 % crystallization and the solidus is at about 700 °C. For the water-rich dacite, crystal content is significantly lower for a given temperature (Fig. 5). The water-rich magma is water-saturated below about 820 °C and has about 5 % water in the melt phase; plagioclase, biotite and magnetite are the only other phases at this temperature. At 780 °C, the mineral assemblage is plagioclase–sanidine–biotite–clinopyroxene–magnetite. Phenocrysts comprise about 34 % of the model magma.

As noted, the natural dacite ignimbrites are phenocryst-rich. If the MELTS calculations are applicable, then a high-H_2O magma with 40 to 55 % crystals would have a temperature of 765 to 710 °C. A low-H_2O magma would have 40 to 50 % crystals at 810 to 740 °C. A variety of mineral geothermometers and experimental data show that the Lund Tuff (as well as other crystal-rich dacites) crystallized at 820 to 735 °C; such high temperatures suggest that the crystal-rich dacites were on the low-H_2O crystallization path. Moreover, water fugacities and mineral resorption patterns reveal that the Lund magma was not water-saturated until after eruption commenced (Christiansen & Best, 1998; Maughan et al. 2001). In addition, the calculated melt water concentration at 50 % crystallinity is in accord with that estimated for crystal-rich dacites by Maughan et al. (2001) and the phase equilibrium experiments of Johnson & Rutherford (1989) on the compositionally similar Fish Canyon Tuff. Thus, the crystallization path for the drier magma (with 2.25 % H_2O) is more applicable to the crystal-rich dacites.
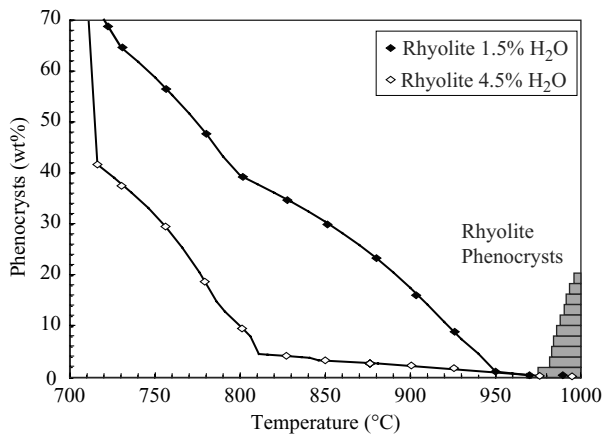
Figure 6. Temperature v. percentage of crystals as calculated for a rhyolitic magma using MELTS (Ghiorso & Sack, 1995). The conditions assumed for the calculations are given in Table 2. The proportions of crystals in the tuff of McMullen Creek (K. Wright, unpub. M.Sc. thesis, Idaho State Univ., 1998) are shown as a histogram on the right.

4.b. Crystallization paths for rhyolite

Similar calculations were performed for rhyolite magma from the Snake River Plain (Fig. 6). The details of the MELTS input parameters are listed in Table 2. The composition of a sample from the tuff of McMullen Creek (K. E. Wright, unpub. M.Sc. thesis, Idaho State Univ., 1998) with 71 % SiO_2 was used in these calculations. The crystallization paths for two different water contents are shown in Figure 6. One set of calculations assumed an initial H_2O content of 1.5 % and the other assumed 4.5 %. For the low-H_2O case, the abrupt increase in the proportion of crystals below 950 °C marks the onset of plagioclase crystallization. At 5 % crystallization, the model melt has a temperature of 950 °C and 1.5 % H_2O. It is in equilibrium with plagioclase and magnetite. Orthopyroxene (920 °C) and sanidine (900 °C) are stable at slightly lower temperatures, but quartz is stable only at temperatures lower than 790 °C. The water-rich magma has much lower calculated crystal contents at any given temperature. At 5 % crystallization the temperature is 810 °C and the magma is water-saturated below 790 °C.

The silicic ignimbrites of the Snake River Plain are generally crystal-poor rhyolite tuffs with 0 to 20 % crystals being typical (Fig. 6). This percentage of phenocrysts occurs in the models for temperatures between about 880 and 1000 °C for water-poor rhyolite and only at much lower temperatures for water-rich rhyolite, temperatures to as low as 780 °C in a water-saturated magma. As noted earlier, eruption temperatures for these crystal-poor rhyolites are high, typically between 850 and 1050 °C, suggesting the 'dry' crystallization conditions are much more likely for the Snake River Plain rhyolites. These eruption/crystallization temperatures are about 100 to 200 °C higher than for the

less silicic, more mafic dacite. This clearly shows that magmatic temperature is not simply correlated with composition and contradicts the typical assumption that rhyolites evolve at lower temperatures than dacites. Tectonic setting is an important control on magmatic temperatures.

5. Viscosity evolution of crystal-bearing dacitic and rhyolitic magma

Armed with these estimates of the initial melt water content and of the relationships between temperature and crystal content for typical dacitic and rhyolitic magma, melt and magma viscosities can be calculated for comparative purposes. The model of Hess & Dingwell (1996) was used to calculate residual melt viscosity as a function of temperature and water content as calculated with MELTS. The effect of crystal content on viscosity was estimated using the Einstein-Roscoe equation as modified by Marsh (1981):

$$\eta_a = \eta(1 - \Phi/\Phi_o)^{-q}$$

where η_a is the apparent magmatic viscosity, η is the viscosity of the compositionally equivalent melt (here corrected for its water content and temperature), Φ is the volume fraction of crystals, Φ_o is the maximum packing fraction of the solid (assumed to be 0.59), and q is a shape and size factor (assumed to equal 2.5). Obviously, this is a rather naive simplification of the viscosity of real crystal-laden magmas, but the calculations serve to compare the two types. For example, estimates of the value of Φ_o range from 0.75 to 0.52. Moreover, viscosities of magmas with crystallinities greater than about 40 % are only approximated by this equation because of the onset of non-Newtonian behaviour (e.g. Lejeune & Richet, 1995). The magmatic viscosity equation used by Spera (2000) is intended to account for melt trapped between crystals and unavailable for shear. It yields bulk magma viscosities that are very similar to those used here, but ranging to 0.5 log units less than calculated with the Einstein-Roscoe equation. The largest deviations are at the highest crystal content, but are not sufficient to change the conclusions.

5.a. Viscosity of melt

The results of the calculations are shown in Figure 7, where melt and magma viscosities are given as a function of temperature. The equation of Hess & Dingwell (1996) predicts that the viscosity of the melt in the dacitic magma is significantly lower than in the rhyolitic magma at a given temperature. Since the melt in both types of magma is rhyolite, the high water content of the melt in the dacite magma causes its lower calculated viscosity. At 800 °C, the melt in the hypothetical dacitic magma has 3.8 wt % H_2O
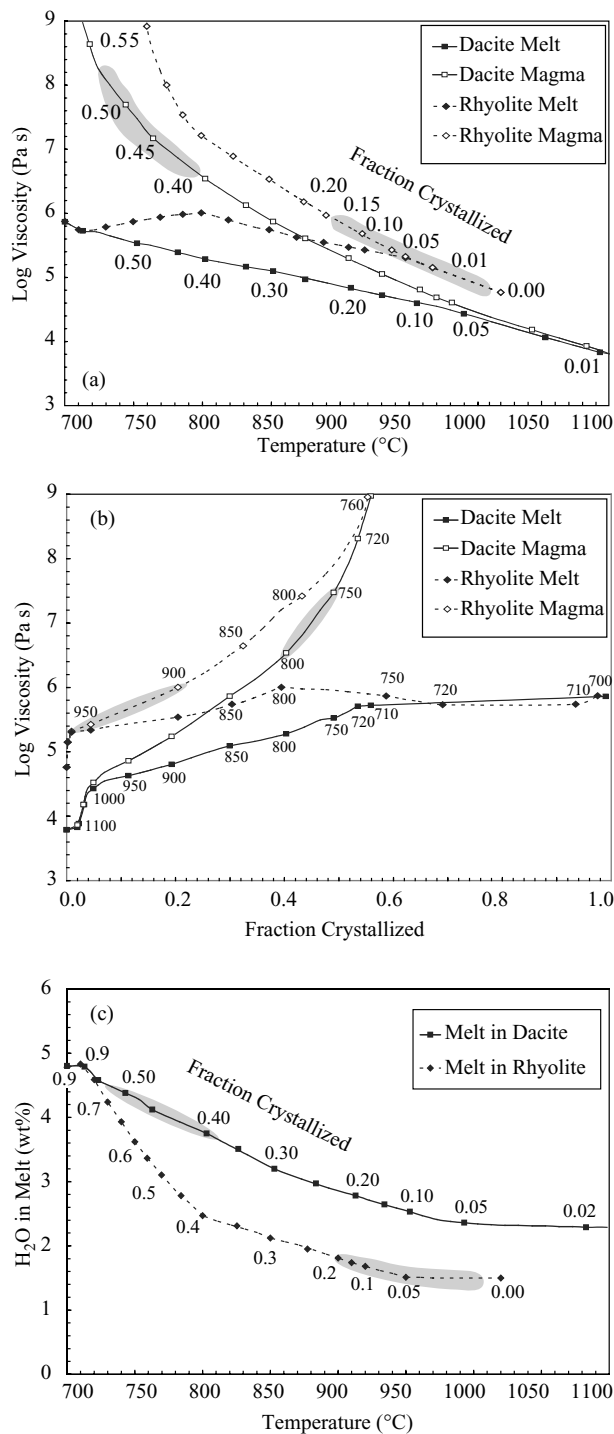
Figure 7. Interrelationships among temperature, viscosity and melt water content for hypothetical rhyolite and dacite magmas. Assumed initial water content was 1.5 % for the rhyolite and 2.25 % for the dacite. Water contents and crystal proportions were calculated with MELTS (Ghiorso & Sack, 1995). See Table 2 for model parameters. Melt viscosities were calculated using the equation of Hess & Dingwell (1996), and magma viscosities were calculated using the Einstein-Roscoe equation (Marsh, 1981). Grey bands show typical values for the distinctive rhyolite and dacite magmas considered here. (a) Magma and melt viscosity v. temperature. Numbers on curves are fraction crystallized. (b) Viscosity v. fraction of crystals. Numbers on curves are temperatures in °C. (c) Melt water content v. temperature. Numbers on curves are fraction crystallized.

and a viscosity of $10^{5.3}$ Pa s, whereas the melt in the rhyolite magma has 2.5 wt % H_2O and a viscosity of 10^6 Pa s. The viscosity of the melt in the dacitic magma continuously decreases at higher temperatures. The rhyolitic melt, on the other hand, has a viscosity maximum of 10^6 Pa s at 800 °C. The maximum marks the onset of quartz crystallization. At temperatures below this, the crystallization rate (ΔXtls/ΔT) is higher and the rate of water enrichment in the residual melt increases until water saturation occurs below 720 °C (Fig. 7c). The enrichment in water is sufficient to lower the viscosity of the melt, even as it cools. In other words, the effect of water on the viscosity of the melt outstrips the effect of lower temperature during this part of the viscosity evolution of the magma.

However, when compared at their typical eruption conditions, the viscosities of the melts in both types of magmas are indistinguishable. For the most common eruption temperatures (925–975 °C for the rhyolites and 750–800 °C for the dacites) the melt viscosities lie in the narrow range between $10^{5.2}$ and $10^{5.5}$ Pa s. The higher temperature of the dry rhyolite melt offsets the viscosity effect of its lower water content. In the dacite, the higher water content of the melt offsets the viscosity effect of the lower temperature of the dacitic magma. Using a similar approach, Clemens & Petford (1999) concluded that leucogranite melts and tonalite melts also have similar viscosities when calculated at reasonable water contents and temperatures.

5.b. Viscosity of magma

Figure 7 also shows the calculated evolution of magma viscosity as a function of temperature, crystallinity and melt water content. The calculated viscosities of the magmas approach infinity as crystal content approaches the value assumed for maximum packing of the crystals (0.59). The viscosity of the water-poor but silica-rich rhyolite magma is about 0.5 log units higher than for the water-rich dacite magma at a given temperature. However, at typical eruption conditions, the dacite magma (with a temperature of 770 °C and 45 % phenocrysts) has a viscosity that is about 1.8 orders of magnitude higher than that of the rhyolite magma (950 °C with 5 % phenocrysts). In spite of higher silica and lower water content, calculated viscosities for the rhyolite magma are significantly lower than for the wetter, but cooler, crystal-rich dacite magma at the conditions under which they erupted. The main reasons for the lower viscosities of the rhyolite magma are its significantly higher temperature and lower crystal contents.

6. Magma chamber processes

The implications of these observations and calculations for the evolution of silicic magma chambers are

manifold. Several authors (e.g. Marsh, 1981; Scaillet *et al.* 1998; Lindsay *et al.* 2001; Bachmann, Dungan & Lipman, 2002) conclude that a significant rheological barrier to magma convection and phenocryst–melt separation occurs at a viscosity of about 10^6 Pa s. The hot-dry rhyolitic magmas are just below this threshold and the cool-wet, but crystal-rich dacite magmas are above it.

Crystal settling is a function of melt viscosity but it is slowed by high proportions of crystals. In crystal-poor rhyolite magma like that modelled here, crystal settling will not be greatly hindered by interference with other crystals. Bachmann & Berganz (2004) calculate that Stokes settling velocity is reduced by about 25 % in magma with 10 % crystals. On the other hand, with 50 % crystals the settling velocity is reduced by about 90 %. In other words, pre-eruptive crystal settling would be about 7 or 8 times faster in crystal-poor rhyolitic magma than in crystal-rich dacitic magma.

Compaction of a crystal mush can expel residual melts and promote differentiation of silicic magma (e.g. Hildreth, 2004). Bachmann & Berganz (2004) concluded that compaction is much less efficient than crystal settling as a means to separate crystals from melt in silicic magma chambers. Moreover, the rate of melt expulsion is inversely related to the fraction of crystals in the melt and to the melt's viscosity. Thus, at typical eruption conditions, it appears that even though the melt viscosities are approximately the same in both rhyolitic and dacitic magma systems considered here, crystal–liquid differentiation by compaction will be much more efficient in the crystal-poor rhyolitic systems than in dacitic systems.

As a consequence of these differences in crystallinity and magma viscosity, two hypothetical magma chambers of the same size and shape might have radically different convection and differentiation histories as described below.

6.a. Cool-wet dacite magma chamber

Shortly before eruption, a monotonous dacite magma may have evolved into a water-rich melt laden with 40 to 50 % crystals with an extremely high viscosity and is near the point where convection and crystal–liquid separation are inefficient if not hindered entirely (Fig. 8). As a consequence of temperature variations in the large magma chamber, various packets of magma would have different crystallinities, different mineral and melt compositions, different densities and different viscosities. Nonetheless, the high crystal load (as well as viscosity and yield strength) of the dacitic magma should strongly hinder the separation of crystals from liquid, either by settling of dense crystals or by compaction-driven flow of buoyant interstitial melt. Crystallization probably proceeded in a quasi-equilibrium fashion in these small domains
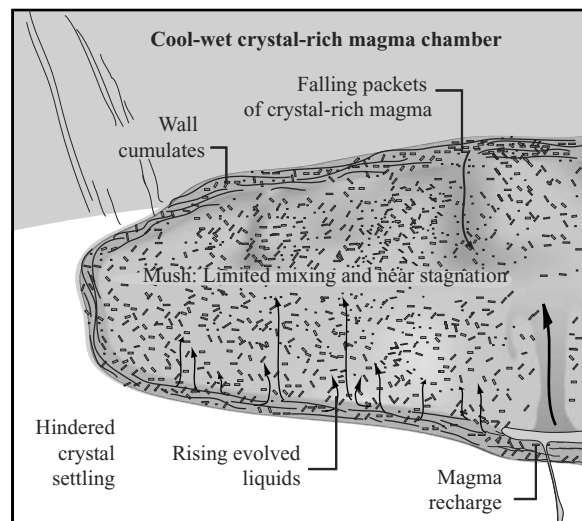

Figure 8. Schematic half-section of a cool monotonous dacite magma chamber. Shortly before eruption, a dacitic magma has evolved into a water-rich melt laden with 40 to 50 % crystals. The viscosity is high enough that separation of crystals from liquids is inefficient if not hindered entirely. Various packets of magma have different temperatures, different mineral and melt compositions, different densities and viscosities. Evolution to high-SiO_2, crystal-poor melt is difficult. Eruption from such a chamber produces a deposit that is dacitic and somewhat variable in composition, but not systematically zoned.

with melts and crystals evolving in composition as temperature changes. Magmatic differentiation of the entire chamber is hindered and vertical systematic zonation may be impossible for these crystal-rich systems. If such a chamber erupts, the deposit should show limited internal variation and lack systematic zonation. Instead, much of the chemical variation in the tuff reflects (1) the extent of crystallization in local packets or domains of magma, (2) mixing of glass and crystals of different compositions during eruption and (3) crystal–glass fractionation during eruption.

6.b. Hot-dry rhyolite magma chamber

On the other hand, water-poor and hot rhyolite magmas may have low enough viscosities to allow efficient crystal–liquid separation (Fig. 9). In a large chamber filled with hot rhyolite magma, even one lacking much water, more efficient separation of crystals from liquids in conjunction with convection appears to create strongly fractionated more highly evolved magmas. Crystallization of cumulates on the walls and floors produces melt that can efficiently escape the crystallization front and accumulate in the centre or roof of the chamber (e.g. Christiansen *et al.* 1988). Zoned plutons may be common in this setting, perhaps analogous to the zoned granites of A-type suites including those in the Baltic Shield (e.g. Rämö & Haapala, 1995; Haapala, 1977). Mixing of evolved residual liquids with less-evolved interior magma
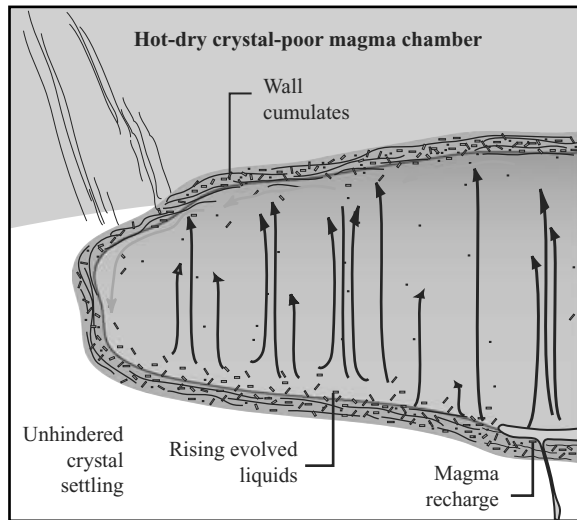
Figure 9. Schematic half-section of a hot-dry rhyolite magma chamber. Before eruption, a silicic magma has differentiated into a highly evolved (or even vertically zoned) chamber because crystal–liquid separation is relatively efficient (and convective fractionation of the melt may proceed). Marginal cumulates drive much of the differentiation. Zoned plutons may be common for this type of magma, analogous to the zoned granites of A-type suites.

should still be a marked feature of such magma systems. Such back-mixing may explain why very large volume rhyolitic ignimbrites are not as strongly zoned as their smaller counterparts erupted from stratovolcanoes.

7. Implications for the growth of large magma chambers and eruption of crystal-rich ignimbrites

If very large volume crystal-rich magmas exist and are convectively dead (or 'moribund' to use Hildreth's (2004) description), why do they erupt to form dacitic ignimbrites? Does water-saturation of the progressively cooling and evolving interstitial melt cause chamber expansion that cracks the roof and drives eruption? Does 'thermal rejuvenation' by hot fluids escaping from subjacent magma (Bachmann, Dungan & Lipman 2002; Bachmann & Bergantz, 2003) somehow trigger eruption? Equally vexing is the question of why such very large volume magmas do not erupt at some 'earlier' stage when they are less chemically evolved and entirely liquid. If several thousand cubic kilometres of andesitic magma differentiating to dacite were emplaced at a shallow level in a molten, near-liquidus state, why are large eruptions (1000s km^3) of andesite or crystal-poor dacite so rare in the eruptive record?

An alternative view holds that a very large crystal-rich dacitic chamber may be the product of protracted growth of a shallow magma system that was never near its liquidus. Rather, magma accumulated sequentially at a rate and temperature that precluded complete cooling or complete melting. Mixing of old residual

magma and new magma would have to be rather efficient. This view contrasts with the emplacement of a near-liquidus magma that progressively cools, crystallizes, assimilates wall rock and differentiates, then stagnates and 'dies' as crystallization brings it to a moribund state.

There is increasing evidence that some plutons and volcanic systems develop over hundreds of thousands to even millions of years with residual magma evolving when new magma is inserted into a dynamic magma chamber (e.g. Hildreth, 1981; Radke, Best & Christiansen, 1992; Huysken, Vogel & Layer, 2001; Vazquez & Reid, 2002; Bachmann, Dungan & Lipman, 2002; Glazner et al. 2004; Coleman, Gray & Glazner, 2004). Figure 10 outlines one possible scenario. Sequential accumulation of smaller batches of magma occurs at a shallow level. Initially the magma cools 'rapidly' against cold wall rock and is largely crystalline. If the ongoing flux of magma is sufficient, complete crystallization is hindered and a crystal-rich magma chamber grows larger and larger. With repeated input, the magma could become less and less crystalline as temperature increases and the fraction of melt grows within the intrusive system (Hirt & Hatton, 2004). Repeated episodes of mixing, melting and crystallizing may mark the magma system's protracted history. Mixing during this stage is a function of Reynolds number and again related to viscosity and crystal content (e.g. Jellinek & Kerr, 1999; Bergantz, 2000). Eventually, as the magma body becomes large and weak (as a consequence of increasing proportion of melt), a critical melt fraction may be reached where the denser roof of the chamber is no longer supported. The inability of the roof to span the great width of the growing magma body may then be a limit to chamber growth. Foundering of the roof into the underlying chamber may trigger a voluminous eruption of crystal-rich magma as volatile-saturation of the interstitial melt follows de-pressurization. Although the existence of a critical melt fraction remains contentious (Petford, 2003), many place the transition from a partially molten solid to a mushy liquid at about 50–55 % crystals (e.g. Marsh, 2000). For example, Lejeune & Richet (1995) show an increase in the effective viscosity of six orders of magnitude between 40 % and 60 % crystallization. Above this critical point, the crystals form a strong interlocking network; below it, viscosity and yield strength drop rapidly (Marsh, 2000). In addition, the transition from Newtonian to non-Newtonian (with significant yield strength) behaviour also lies between 30 % and 50 % crystals (Petford, 2003). These important rheological transitions occur near the crystallinity of the very large volume dacites considered here.

On the other hand, hot crystal-poor rhyolites may have originated as crystal-poor melts either by efficient fractionation of hot basaltic magma (e.g. Nekvasil et al. 2004) or by clean separation of hot, low viscosity

Very large volume
ignimbrite fills caldera

(f)

Very large eruption
of pyroclastic flows

Roof collapses into
weak, melt-enriched
chamber

(e)

Fractures form and support of roof drops

Continued uplift

Growth of
chamber

More molten

Subsidence below
chamber

(d)

Uplift of surface

Continued growth of
mushy magma chamber
More molten

(c)

Magma nearly stagnant
Little differentiation

Continued growth of
mushy magma chamber
More molten

(b)

10 km

Evolution of a large-volume dacitic magma system

Small chamber, cools
quickly, mostly solid

Rising mafic recharge and
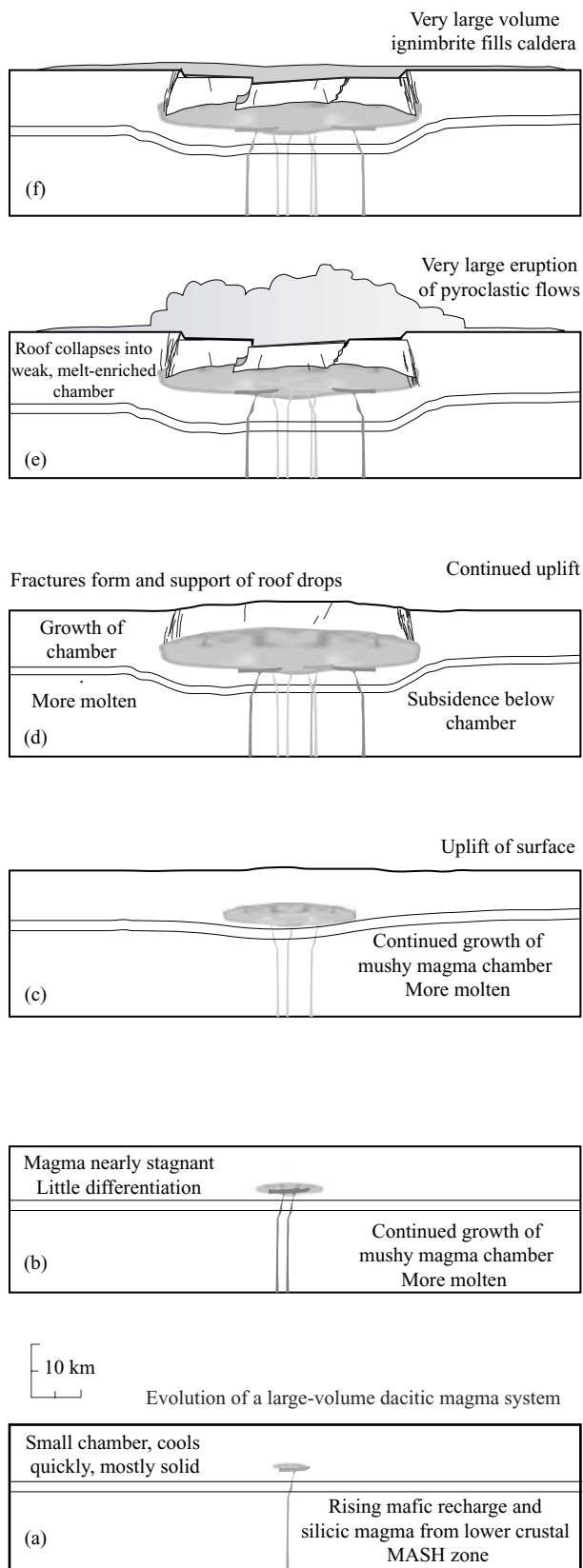silicic magma from lower crustal
MASH zone

(a)

Figure 10. The evolution of a dacitic magma system over an approximately 1 million year time period is shown in this series of cross-sections. Early intrusions of magma cool quickly and are largely solid (a). Sequential additions (b, c) to the shallow magma chamber lead to a larger and increasingly molten body of magma. If the chamber grows and the proportion of melt

($< 10^{4.5}$ Pa s; see Fig. 7) partial melt of basaltic crust (Frost & Frost, 1997). Repeated eruptions may be driven by the inability of the roof to span a large magma chamber and its subsequent collapse.

8. Conclusions

The model presented here only explains two rather extreme end-members of a spectrum of magma composition–volume–temperature relations. Of course, this model does not explain the origin of crystal-rich calc-alkaline rhyolites such as the Joy Tuff, Dell Tuff and other crystal-rich rhyolitic ignimbrites of the Great Basin (Lindsey, 1981; D. V. Walsh, unpub. M.Sc. thesis, Univ. Iowa, 1987). They are chemically and mineralogically similar to other high-K continental margin rhyolites around the world and have smaller volumes than those considered here. On the other hand, some cool, relatively crystal-poor rhyolite tuffs erupted in the Great Basin and the central Andes between eruptions of the very large volume dacites (Best, Christiansen & Blank, 1989; Lindsay *et al.* 2001). Compaction of crystal-rich dacitic magma or gas-sparging (e.g. Bachman & Bergantz, 2003, 2004) may have played roles in creating smaller volumes of crystal-poor rhyolites found in conjunction with very large volume crystal-rich dacites. Moreover, the conclusions must be tempered with the knowledge that the viscosity estimates are limited by the range of existing experiments and by the simplifying assumptions made (e.g. the value of the critical melt fraction and the constancy of the power law exponent).

Given these limitations, the main conclusion of this paper is that large variations in magma viscosity (10^4 to 10^9 Pa s) correlate largely with crystal content. This contrasts with the findings of Scaillet, Holtz & Pichavant (1998) and Clemens & Petford (1999), who concluded that silicic magmas have rather constant viscosity of about $10^{4.5}$ Pa s, based largely on the assumption that magmas are extracted from their sources, emplaced and differentiated at their liquidus temperatures.

If very large volumes of hot, water-poor rhyolite with low phenocryst proportions and low enough viscosities ($< 10^6$ Pa s) exist, then efficient crystal–liquid separation can occur. Differentiation of such magma is probably by floor and sidewall crystallization. Strong compositional evolution by fractional crystallization is characteristic of such magmas. Some of these crystal-poor rhyolite chambers become vertically zoned by sidewall crystallization and the rise of fractionated,

increases, the magma becomes weaker and ultimately, perhaps at a critical melt fraction near 50 % (d), it may be unable to support the denser roof of the chamber. The roof collapses (e) and triggers eruption of the crystal-rich dacitic magma. The caldera is partially filled and surrounded by crystal-rich ignimbrite (f).

less-dense magma to the top of large chambers. Vertical zonation may not be as efficient as in smaller chambers because zonation in larger, flatter chambers may be hindered by back-mixing. These features (hot and water-poor magmas) are best developed in A-type silicic magmas related to hotspots where large fluxes of hot, volatile-poor magma is extracted from the mantle and emplaced in the crust.

Monotonous dacites are very large volume ignimbrites that are consistently water-enriched and cool by comparison to the hot, dry rhyolites described here. The dacites have abundant (40 to 50 %) phenocrysts and high viscosities ($> 10^6$ Pa s). The high crystallinity and viscosity of the water-rich but cool magma makes crystal fractionation inefficient. Instead, it promotes quasi-equilibrium crystallization in small domains within a large heterogeneous magma chamber. This characteristic also inhibits development of pronounced vertical zonation of the magma body. Monotonous dacites are favoured in continental subduction regimes where the underthrust slab breaks off or steepens over the course of a few million years (e.g. Maughan *et al.* 2001; Best & Christiansen, 1991). This produces large volumes of wet mantle-derived magma that can indirectly fuel shallow magma systems. Furthermore, the eruptive characteristics and inferred crystallization histories imply that this type of crystal-rich dacitic magma was never near its liquidus. These dacitic magmas may have evolved by the accumulation of multiple injections of mushy magma sustained over hundreds of thousands of years. Eruptions may have been triggered when the roof of the evolving chamber could no longer span a growing intrusion filled with increasingly weaker, more melt-rich magma.

References

BACHMANN, O. & BERGANTZ, G. W. 2003. Rejuvenation of the Fish Canyon magma body: A window into the evolution of large-volume silicic magma systems. *Geology* **31**, 789–92.

BACHMANN, O. & BERGANTZ, G. W. 2004. On the origin of crystal-poor rhyolites: Extracted from batholithic crystal mushes. *Journal of Petrology* **45**, 1565–82.

BACHMANN, O. & DUNGAN, M. A. 2002. Temperature-induced Al-zoning in hornblendes of the Fish Canyon magma, Colorado. *American Mineralogist* **87**, 1062–76.

BACHMANN, O., DUNGAN, M. A. & LIPMAN, P. W. 2002. The Fish Canyon magma body, San Juan volcanic field, Colorado: Rejuvenation and eruption of an upper-crustal batholith. *Journal of Petrology* **43**, 1469–1503.

BERGANTZ, G. W. 2000. On the dynamics of magma mixing by reintrusion: implications for pluton assembly processes. *Journal of Structural Geology* **22**, 1297–1309.

BEST, M. G., CHRISTIANSEN, E. H. & BLANK, H. R. JR. 1989. Oligocene caldera complex and calc-alkaline tuffs and lavas of the Indian Peak volcanic field, Nevada and Utah. *Geological Society of America Bulletin* **101**, 1076–90.

BEST, M. G. & CHRISTIANSEN, E. H. 1991. Limited extension during peak Tertiary volcanism, Great Basin of Nevada and Utah. *Journal of Geophysical Research* **96**, 13509–28.

CATHEY, H. E. & NASH, B. P. 2004. The Cougar Point Tuff: Implications for thermochemical zonation and longevity of high-temperature, large-volume silicic magmas of the Miocene Yellowstone hotspot. *Journal of Petrology* **45**, 27–58.

CHRISTIANSEN, E. H. & BEST, M. G. 1998. Resorption of quartz, sanidine, and plagioclase phenocrysts in silicic ash-flow tuffs as a result of decompression. *EOS* **79**(45), F925.

CHRISTIANSEN, E. H., STUCKLESS, J. S., FUNKHOUSER, M. J. & HOWELL, K. A. 1988. Petrogenesis of rare-metal granites from depleted crustal sources – an example from the Cenozoic of western Utah, USA. In *Recent advances in the geology of granite-related mineral deposits* (eds R. P. Taylor and D. F. Strong), pp. 307–21. *Canadian Institute of Mining and Metallurgy Special Volume* **39**.

CHRISTIANSEN, R. L. 2001. The Quaternary and Pliocene Yellowstone Plateau volcanic field of Wyoming, Idaho, and Montana. Geology of Yellowstone National Park. *U. S. Geological Survey Professional Paper* **729–G**, 145 pp.

CLEMENS, J. D. & PETFORD, N. 1999. Granitic melt viscosity and silicic magma dynamics in contrasting tectonic settings. *Journal of the Geological Society, London* **156**, 1057–60.

COLEMAN, D. S., GRAY, W. & GLAZNER, A. F. 2004. Rethinking the emplacement and evolution of zoned plutons: Geochronologic evidence for incremental assembly of the Tuolumne Intrusive suite, California. *Geology* **32**, 433–6.

COSTA, R., SCAILLET, B. & PICHAVANT, M. 2004. Petrological and experimental constraints on the pre-eruption conditions of Holocene dacite from Volcan San Pedro (36°S, Chilean Andes) and the importance of sulphur in silicic subduction-related magmas. *Journal of Petrology* **45**, 855–81.

DESILVA, S. L. & WOLFF, J. A. 1995. Zoned magma chambers: The influence of magma chamber geometry on sidewall convective fractionation. *Journal of Volcanology and Geothermal Research* **65**, 111–18.

EKREN, E. B., ANDERSON, R. E., ROGERS, C. L. & NOBLE, D. C. 1971. Geology of the northern Nellis Air Force Base Bombing and Gunnery Range, Nye County, Nevada. *U.S. Geological Survey Professional Paper* **651**, 91 pp.

FRANCIS, P. W., SPARKS, R. S. J., HAWKESWORTH, C. J., THORPE, R. S., PYLE, D. M., TAIT, S. R., MANTOVANI, M. S. & MCDERMOTT, F. 1989. Petrology and geochemistry of volcanic rocks of the Cerro Galan caldera, northwest Argentina. *Geological Magazine* **126**, 515–47.

FROST, B. R., BARNES, C. G., COLLINS, W. J., ARCULUS, R. J., ELLIS, D. J. & FROST, C. D. 2001. A geochemical

classification for granitic rocks. *Journal of Petrology* **42**, 2033–48.

FROST, C. D. & FROST, B. R. 1997. Reduced rapakivi-type granites: The tholeiite connection. *Geology* **25**, 647–50.

GHIORSO, M. S. & SACK, R. O. 1995. Chemical mass transfer in magmatic processes IV. A revised and internally consistent thermodynamic model for the interpolation and extrapolation of liquid-solid equilibria in magmatic systems at elevated temperatures and pressures. *Contributions to Mineralogy and Petrology* **119**, 197–212.

GLAZNER, A. F., BARTLEY, J. M., COLEMAN, D. S., GRAY, W. & TAYLOR, R. Z. 2004. Are plutons assembled over millions of years by amalgamation from small magma chambers? *Geology Today* **14**, 4–11.

HAAPALA, I. 1977. Petrography and geochemistry of the Eurajoki stock; a rapakivi-granite complex with greisen-type mineralization in southwestern Finland. *Bulletin of the Geological Society of Finland* **286**, 128 pp.

HESS, K. & DINGWELL, D. B. 1996. Viscosities of hydrous leucogranitic melts: A non-Arrhenian model. *American Mineralogist* **81**, 1297–1300.

HILDRETH, W. 1981. Gradients in silicic magma chambers: Implications for lithospheric magmatism. *Journal of Geophysical Research* **86**, 10153–92.

HILDRETH, W. 2004. Volcanological perspectives on Long Valley, Mammoth Mountain, and Mono Craters: several contiguous but discrete systems. *Journal of Volcanology and Geothermal Research* **136**, 169–98.

HILDRETH, W., HALLIDAY, A. N. & CHRISTIANSEN, R. L. 1991. Isotopic and chemical evidence concerning the genesis and contamination of basaltic and rhyolitic magma beneath the Yellowstone Plateau volcanic field. *Journal of Petrology* **32**, 63–138.

HIRT, W. H. & HATTON, J. R. 2004. Thermal modeling of a composite felsic intrusion: Implications for the origin of compositional zoning within members of the Mount Whitney Intrusive Suite, Sierra Nevada, California. *Geological Society of America, Abstracts with Programs* **36**.

HUYSKEN, K. T., VOGEL, T. A. & LAYER, P. W. 2001. Tephra sequences as indicators of magma evolution; ^{40}Ar/^{39}Ar ages and geochemistry of tephra sequences in the Southwest Nevada volcanic field. *Journal of Volcanology and Geothermal Research* **106**, 85–110.

JELLINEK, A. M. & KERR, R. C. 1999. Mixing and compositional stratification produced by natural convection: 2. Applications to the differentiation of basaltic and silicic magma chambers and komatiite lava flows. *Journal of Geophysical Research* **104**, 7203–18.

JOHNSON, M. C. & RUTHERFORD, M. J. 1989. Experimentally determined conditions in the Fish Canyon tuff, Colorado, magma chamber. *Journal of Petrology* **30**, 711–37.

LINDSAY, J. M., SCHMITT, A. K., TRUMBULL, R. B., DESILVA, S. L., SIEBEL, W. & EMMERMANN, R. 2001. Magmatic evolution of the La Pacana caldera system, central Andes, Chile: Compositional variation of two cogenetic, large-volume felsic ignimbrites. *Journal of Petrology* **42**, 459–86.

LINDSEY, D. A. 1981. Tertiary volcanic rocks and uranium in the Thomas Range and northern Durm Mountains, Juab County, Utah. *U. S. Geological Survey Professional Paper* **1221**, 71 pp.

LEJEUNE, A. M. & RICHET, P. 1995. Rheology of crystal-bearing silicate melts: an experimental study at high viscosities. *Journal of Geophysical Research* **100**, 4215–19.

MARSH, B. D. 1981. On the crystallinity, probability of occurrence, and rheology of lava and magma. *Contributions to Mineralogy and Petrology* **78**, 58–98.

MARSH, B. D. 2000. Magma chambers. In *Encyclopedia of volcanoes* (ed. H. Sigurdsson), pp. 191–206. San Diego: Academic Press.

MASON, B. G., PYLE, D. M. & OPPENHEIMER, C. 2004. The size and frequency of the largest explosive eruptions on Earth. *Bulletin of Volcanology* **66**, 735–48.

MAUGHAN, L., CHRISTIANSEN, E. H., BEST, M. G. & GROMME, S. 2001. The Oligocene Lund Tuff, Great Basin, USA: A very large volume monotonous intermediate. *Journal of Volcanology and Geothermal Research* **113**, 129–57.

NEKVASIL, H., DONDOLINI, A., HORN, J., FILIBERTO, J., LONG, H. & LINDSLEY, D. H. 2004. The origin and evolution of silica-saturated alkalic suites: an experimental study. *Journal of Petrology* **45**, 693–721.

PERKINS, M. E. & NASH, W. P. 2002. Explosive silicic volcanism of the Yellowstone Hotspot; the ash fall tuff record. *Geological Society of America Bulletin* **114**, 367–81.

PETFORD, N. 2003. Rheology of granitic magmas during ascent and emplacement. *Annual Reviews of Earth and Planetary Science* **31**, 399–427.

RADKE, L. E., BEST, M. G. & CHRISTIANSEN, E. H. 1992. Petrology and temporal evolution of the rhyolite ash-flow tuffs of the 35. 4 Ma Stone Cabin Formation, central Nevada. *EOS* **73**(43), 623.

RÄMÖ, O. T. & HAAPALA, I. 1995. One hundred years of rapakivi granite. *Mineralogy and Petrology* **52**, 29–185.

ROSS, K. T., CHRISTIANSEN, E. H., BEST, M. G., DORAIS, M. J. & TINGEY, D. G. 2002. Petrology and emplacement of the Cottonwood Wash Tuff. *Geological Society of America Abstracts with Programs* **34**(3), 9.

SCAILLET, B., HOLTZ, F., PICHAVANT, M. & SCHMIDT, M. 1998. Viscosity of Himalayan leucogranites: Implications for mechanisms of granitic magma ascent. *Journal of Geophysical Research* **101**, 27691–9.

SCAILLET, B., HOLTZ, F. & PICHAVANT, M. 1998. Phase equilibrium constraints on the viscosity of silicic magmas: 1. Volcanic-plutonic comparison. *Journal of Geophysical Research* **103**, 27257–66.

SPERA, F. J. 2000. Physical properties of magmas. In *Encyclopedia of volcanoes* (ed. H. Sigurdsson), pp. 171–90. San Diego: Academic Press.

VAZQUEZ, J. A. & REID, M. R. 2002. Time scales of magma storage and differentiation of voluminous high-silica rhyolites at Yellowstone caldera, Wyoming. *Contributions to Mineralogy and Petrology* **144**, 274–85.

WHITNEY, J. A. & STORMER, J. C. 1985. Mineralogy, petrology, and magmatic conditions from the Fish Canyon Tuff, central San Juan Volcanic Field, Colorado. *Journal of Petrology* **26**, 726–62.

WRIGHT, K. E., MCCURRY, M. & HUGHES, S. S. 2002. Petrology and geochemistry of the Miocene Tuff of McMullen Creek, central Snake River Plain, Idaho, In *Tectonic and Magmatic Evolution of the Snake River Plain Volcanic Province* (eds B. Bonnichsen, C. M. White and M. McCurry), pp. 177, 194. Idaho Geological Survey Bulletin.